Computer Vision Applied to 3D Medical Images: Results, Trends and Future Challenges

Nicholas Ayache

Computer Vision Applied to 3D Medical Images: Results, Trends and Future Challenges

Nicholas Ayache
INRIA
B.P. 93
06902 Sophia-Antipolis, France
Email: ayache@sophia.inria.fr

Abstract

The automated analysis of 3D medical images can improve significantly both diagnosis and therapy. This automation raises a number of new fascinating research problems in the fields of computer vision and robotics.

In this paper, I propose a list of such problems after a review of the current major 3D imaging modalities, and a description of the related medical needs.

I then present some of past and current work done in the research group EPIDAURE[1] at INRIA, on the following topics: segmentation of 3D images, 3D shape modeling, 3D rigid and nonrigid registration, 3D motion analysis and 3D simulation of therapy.

Most topics are discussed in a synthetic manner, and illustrated by results. Rigid Matching is treated more thoroughly as an illustration of a transfer from computer vision towards 3D image processing. Last topics are illustrated by preliminary results and suggest a number of promising research tracks and future challenges.

Keywords: Volume Image Processing, Medical Images, 3D Vision, Medical Robotics, Research Trends.

1 Introduction

1.1 New Images

Three-dimensional (3D) images are becoming very popular in the medical field [54], [116], [96], [11], [120]. A modern hospital commonly produces every year tens of thousands of volumetric images. They come from different modalities like Magnetic Resonance Imagery (**MRI**),Computed Tomography Imagery (**CTI**, also called Scanner Imagery), Nuclear Medicine Imagery (**NMI**) or Ultrasound Imagery (**USI**).

These images share the particularity of describing the physical or chimical properties at each point of a studied **volume**. These informations are stored in a discrete 3D matrix $I(i,j,k)$ of voxels (volume elements), called a 3D image because of the analogy with digital 2D images $I(i,j)$ stored as 2D matrices of pixels (picture elements). Actually, the most simple exploitation of 3D images consists in a direct visualization of the successive 2D images (also called cross-sections) obtained by setting one of the 3 coordinates (i,j,k) to a constant. In fact, applying advanced 3D image processing and graphics allow much more vivid and realistic displays, as it is shown in figure 1, built from a 3D MRI whose figure 2 shows a few cross-sections.

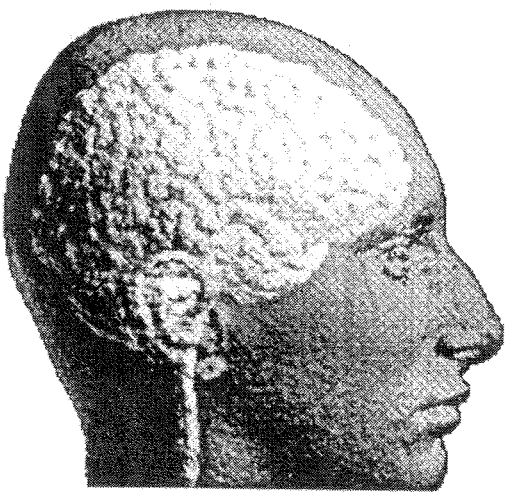

Figure 1: A 3D display of two well known anatomical structures extracted automatically from a single 3D Magnetic Resonance Image (MRI) of the head. The automatic extraction and display of these structures involves advanced 3D image processing.

Cross-sections from the 4 main imaging modalities are shown in Figure 3. In MRI, the intensity I measures locally the density and structures of protons, while in CTI, intensity measures locally the density of X-ray absorbtion. CTI and MRI provide complementary **anatomical** informations. CTI gives very contrasted images of the bones, while MRI gives excellent descriptions of most organs and soft tissues, as well as a reasonably good description of the bones.

[1] EPIDAURE is a very nice location in Greece which used to be the sanctuary of ancient medicine. Today, for computer scientists, it is also a recursive acronym (in French): *Epidaure, Projet Image, Diagnostic A Utomatique, et RobotiquE.*

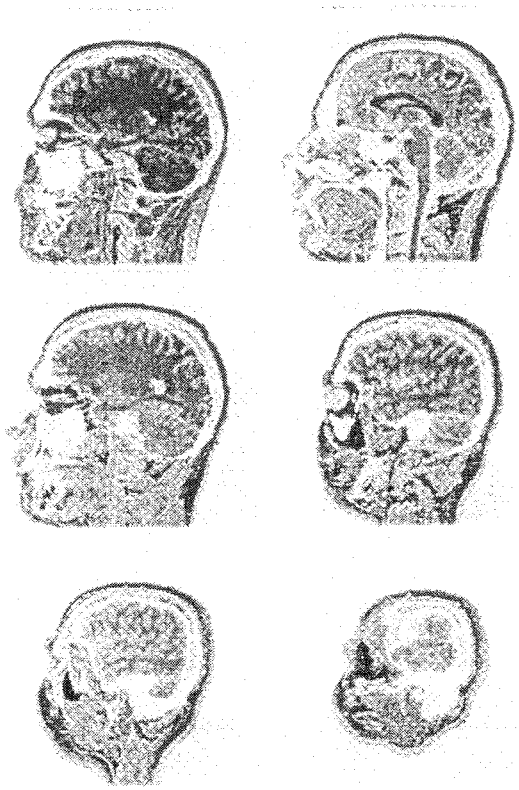

Figure 2: A few cross-sections extracted from a 3D MRI image of the head

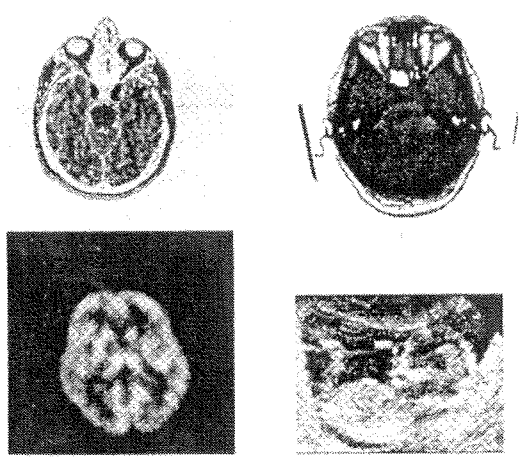

Figure 3: 4 different modalities of acquisition of 3D images: MRI, CTI, NMI and USI. Although each image is produced 3 dimensions, only one cross-section is shown here. First 3 images show the head, the last one a young foetus (7cm!).

NMI measures locally the density of some injected radio-active molecules. It therefore provides a **functional** information on the metabolism of the studied regions (e.g. the density of glucose used per unit of time and volume in the brain). Major sources of NMI are Single Photon Emission Computed Tomography (SPECT), while Positon Emission Tomography (PET) is still a research tool.

Finally, USI measures locally the variation of the acoustic impedance (a function of the speed of ultrasound propagation). Although most commonly used in 2 dimensions, ultrasound images can also be acquired in 3D [58], [39]. Ultrasound images are easily acquired at a very fast rate, giving both **anatomical** information (boundaries of anatomical structures usually correspond to variations of the acoustic impedance), and **dynamic** informations (e.g. the heart motion). Dynamic information can also be obtained by gated (i.e. synchronized) MRI or NMI.

Although USI and MRI are recognized as non-invasive (non dangerous) techniques, this is not the case for CTI and NMI which involve radio-active materials. Prices of equipments vary a lot from one modality to another: currently the cheapest is USI (typically less than 100 k$), while the most expensive is MRI (typically several M$).

New 3D imagery devices are emerging, like angiographic MRI, which describes the anatomy of the vascular system, magneto-encephalography equipment, which measures magnetic field variations, or functional MRI, which provides metabolism informations (like NMI), but with a non invasive method. These new modalities are still in the research stage, but might lead to major 3D imaging devices in the near future.

1.2 New Markets

The market of the **production** of medical images was evaluated to 8 billion of US dollars in 1991 [100], [35], and shows approximately an increase of 10% per year. Among these figures, MRI represents currently a market of 1 billion dollars, with a strong increase of approximately 20% per year [84].

Besides the production itself, 3D image **processing** is the most recent market. Almost inexistent a few years ago, it is evaluated to 350 million dollars in 1992, with a planned evolution between 20 and 40% per year during the next 5 years.

This comes from the new capabilities demonstrated by computer vision applied to 3D imagery. Not only it provides better diagnosis tools, but also new possibilities for therapy. This is true in particular for brain and skull surgery, laparoscopy and radiotherapy, where simulation tools can be tested in advance, sometimes with the help of virtual reality, and used during the intervention as guiding tools [62], [39], [93]. In some cases, even robots can use pre-operative and per-operative 3D imagery to complete precisely some specific medical gestures prepared during a simulation phase [94], [69].

One must notice that 3D imagery is also in expansion in other fields than medical. In **biology**, confocal microscopy produces voxel images at a microscopic scale. In the **industry**, non destructive inspection of important parts like turbine blades for instance is sometimes made with CTI. Finally, in **geology**, large petroleum companies like Elf-Aquitaine for instance, have bought scanners (CTI) to analyse core samples.

1.3 New Medical Needs

Exploiting 3D images in their raw format (a 3D matrix of numbers) is usually a very akward task. For instance, it is now quite easy to acquire MRI images of the head with a resolution of about a millimeter in each of the 3 directions. Such an image can have 256^3 voxels, which represent about 17 Megabytes of data. High resolution 3D images of the heart can also be acquired during a time sequence, which represent spatio-temporal data in 4 dimensions. In both cases, displaying 2D cross-sections one at a time is no longer sufficient to establish a reliable diagnosis or prepare a critical therapy.

Moreover, the complexity of the anatomical structures can make their identification difficult, and the use of multimodal complementary images requires accurate spatial registration. Long term study of a patient evolution also requires accurate spatio-temporal registration.

We identified the automation of the following tasks as being crucial needs for diagnosis and therapy improvement:

1. **Interactive Visualization** must be really 3D, with dynamic animation capabilities. The result could be seen as a flight simulation within the anatomical structures of a human body. A recent review of the state of the art can be found in [104].

2. **Quantification** of **shapes**, **textures** and **motion** must provide the physician with a reduced set of parameters useful to establish his diagnosis, study temporal evolution, and make inter-patient comparisons. This must be true for the analysis of static and dynamic images.

3. **Registration** of 3D images must be possible for a given patient between single or multi-modality 3D images. This spatial superposition is a necessary condition to study in great details the evolution of a pathology, or to take full advantage of the complementarity information coming from multimodality imagery. Extensions to the multi-patient cases is also useful, because it allows subtle inter-patient comparisons.

4. **Identification** of anatomical structures within 3D images requires the construction of computerized anatomical atlases, and the design of matching procedures between atlases and 3D images. Such a registration would provide a substantial help for a faster interpretation of the most complex regions of the body (e.g. the brain), and it is a prerequisite to solve the previous multi-patient registration problem, and to help planification (see below).

5. **Planification, Simulation and Control** of therapy, especially for delicate and complex surgery (e.g. brain and crano-facial surgery, hip, spine and eye surgery, laparoscopy ...), and also for radiotherapy: this is an ultimate goal. The therapist, with the help of interactive visualization tools applied to quantified, registered and identified 3D images, could planify in advance its intervention, taking advantage of a maximum of planification advices, and then observe and compare predicted results before any operation is done. Once the best solution is chosen, the actual intervention could then be controlled by passive or active mechanical devices, with the help of per-operative images and other sensors like force sensors for instance.

1.4 New Image Properties

To fulfill these medical needs, it is necessary to address a number of challenging new computer vision and robotics problems [3], [43]. Most of these problems are quite new, not only because images are in three dimensions, but also because usual approximations like polyhedral models or typical assumptions like rigidity rarely apply to medical objects. This opens a large range of new problems sometimes more complex than their counterparts in 2D image analysis.

On the other hand, specific properties of 3D medical imagery can be exploited very fruitfully. For instance, contrary to video images of a 3D scene, geometric measurements are not projective but **euclidean measurements**. Three dimensional coordinates of structures are readily available!

Moreover, one can usually exploit the **intrinsic value of intensity**, which is generally related in a simple way to the physical or physiological properties of the considered region: this is almost never the case with video images where intensity varies with illumination, point of view, surface orientation etc...)

Also, **a priori knowledge** is high, in the sense that physicians usually have protocols (unfortunately depending on the image modality) to acquire images of a given part of the body, and different patients tend to have similar structures at similar locations!

Finally, having a dense set of **3D data** provides a better local regularization when computing local differential properties, as we shall see later.

1.5 New Computer Vision and Robotics Issues

Having listed the medical needs and the new image properties, I now set a list of computer vision and robotics issues which we believe are central problems :

1. **3D Segmentation** of images: the goal is to partition the raw 3D image into regions corresponding to meaningful anatomic structures. It is a prerequisite to most of the medical needs listed before. Efficient segmentation requires the modeling and extraction of 3D static or dynamic edges and of 3D texture, as well as the generalization of 2D digital topology and mathematical morphology in 3D.

2. **3D Shape Modeling**: this is mainly a prerequisite to solve the registration and identification needs, but also for efficient visualization. It is necessary to describe non-polyhedral 3D shapes with a reduced number of intrinsic features. This involves mainly computational and differential geometry.

3. **3D Matching** of 3D shapes: once segmented and modeled, new algorithms must be designed to reliably and accurately match such representations together, both in rigid and nonrigid cases. This is necessary to solve the registration and identification needs.

4. **3D Motion Analysis**: this requires the development of new tools to process sequences of 3D im-

ages, (i.e. 4D images!), in order to track and describe rigid and nonrigid motion of 3D anatomical structures. This is necessary for the quantification of motion needs.

5. **Dynamic Physical Models** of anatomical structures should be developped to provide realistic simulation of interaction with 3D images. This is required for the planification and simulation of therapy. Physical models can also help solving the previous 3D motion analysis problems.

6. **Geometric Reasoning** is required to help therapeutic planification, in particular to determine trajectories of beam sources in radiotherapy, and succession of accurate medical gestures in surgery.

7. **Virtual Reality** environment should be developped to provide realistic interactive visualization and to help planification and simulation.

8. **Dedicated Medical Robots**, possibly passive or semi-active, equiped with specific sensors (force sensing, optical or ultrasound positioning, ...), must be developped for the automatic control of therapy.

As one should notice, these problems are mainly computer vision and robotics problems, involving also graphics. In the following, I address them (except the last one, but see Taylor-et-al's paper in these proceeding for a spectacular example of a dedicated medical robot) by presenting the research conducted during the past 4 years in the research group EPIDAURE at INRIA. I present the basic lines of this research, the main results, and try to indicate some promising research tracks. References go primarily to the papers published by the EPIDAURE group, although I tried to add a significant (but necessarily incomplete!) list of complementary references.

2 Segmentation of 3D images

Segmentation of 3D images has similarities with the classical problem of segmenting 2D images. The purpose is the same, namely to partition the original set of image points into subsets corresponding to meaningful objects. As for 2D image processing, both region-based and contour-based approaches apply, with the specificity that regions are now volumes and that edges become surfaces.

We found that a set of generic tools were quite effective to solve completely a number of specific segmentation problems both in static and dynamic images. These include 3D edge extraction, 3D digital topology and mathematical morphology operators, 2D and 3D active contours, and 3D texture analysis tools. We found that combined together these tools could solve the problem of segmenting major anatomical structures in CTI and MRI, and also the tracking of 2D and 3D structures of the beating heart in dynamic USI and NMI [4].

2.1 3D Edges

As previously mentionned, a major advantage of 3D images comes from the fact that intensity is usually a simple function of the studied structures (contrary to video images of a 3D scene). To segment CTI or MRI images, assuming constant intensity plus additive noise within a given anatomical structure is often a reasonable assumption in regions with low texture. Intensity in NMI images is also simply related to the physiological function studied, but the resolution is often lower with a higher noise level. The most difficult images to segment are probably USI, where intensity already measures a function of the derivative of the acoustic impedance of the tissues, but with a strong multiplicative (in frequency domain) noise producing a very typical "speckle" texture almost everywhere.

For regions with low texture, O. Monga [88], [89] showed that the 3D generalization of the Deriche-Canny edge operator [32] was quite efficient to extract edges. The superiority of 3D filtering the volumetric data instead of successively filtering 2D cross-sections was clearly demonstrated as can be seen in figure 4.

Figure 4: 3D edge detection is more robust and coherent than 2D edge detection: left, we show the result of 2D edge detection performed in successive cross-sections which were orthogonal to the plane of the picture. Result from one cross-section to the next is not as coherent as it is with 3D edge filtering (right) where none of the 3 principal directions is privileged. (Courtesy of G. Malandain and O. Monga)

Because 3D filtering is computationally more intensive, the use of separable recursive filters is crucial for the sake of computational complexity. G. Malandain implemented a version of the 3D edge detector which has been distributed to several places.

2.2 Digital Topology, and Mathematical Morphology

Thresholding and/or edge detection must generally be followed by some 3D mathematical morphology oper-

ators (erosion, dilation, thinning, connected component analysis...) to separate regions from one another. These operations require a formal analysis of the discrete notions of connectivity for points, curves, surfaces and volumes in 3D images. This is the purpose of digital topology [53], [65], and mathematical morphology [101], disciplines to which G. Malandain and G. Bertrand brought recently interesting new results and algorithms [77], [13]. For instance, they show in figure 5 the extraction of topological singularities on the surface of 2 skulls.

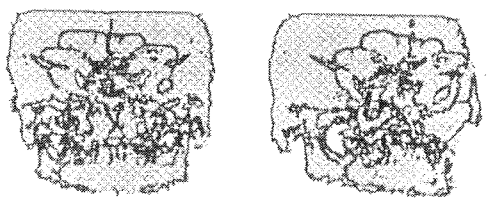

Figure 5: shows the extraction of topological singularities on the surface of 2 skulls. One should note the remarkable stability of these lines, which can be used for registration. (Courtesy of G. Malandain and G. Bertrand)

2.3 Deformable Surfaces

This approach consists in generalizing in 3 dimensions the active contours introduced by Kass, Witkin and Terzopoulos [61], [106]. A variational method has been developped by Laurent Cohen and then by Isaac Cohen to minimize an energy which accounts for the elasticity properties of the surface (internal energy) and the proximity of detected edgeis (external energy). The mathematical framework is the one of the finite elements, which provides a sound and stable analytical description of the surface. This approach provides a good segmentation of simple surfaces with a simple topology [22], [20], [23].

We show in figures 6 an example of the segmentation of a heart ventricle in a 3D image. After the segmentation of such a 3D image, deformable surfaces appear to be very efficient to track a deformable structure in a time sequences of 3D images [5]. Connected work can be found in [108], [25], [49], [75], [42], [71], [81], [80], [29], [76], [99].

2.4 Sonar Space Filtering

In some cases, it might be interesting to perform the segmentation before 3D image reconstruction, i.e. from the raw data obtained by the original sensor. This was clearly demonstrated for USI, with a method called Sonar Space Filtering.

In USI, I. Herlin and R. Vojak showed that the polar geometry of USI requires a special type of filtering which computes edges at the local resolution of the raw data. This is important, because once the image is rectified from polar to cartesian coordinates, some information is lost, and the edge extraction results are degraded. Results are good enough in time sequences of echographic images to analyse the motion of the mitral valve of the heart, with the help of the previous active contours [50] [51]. Similar results are also obtained by I. Herlin with Markov random fields [52].

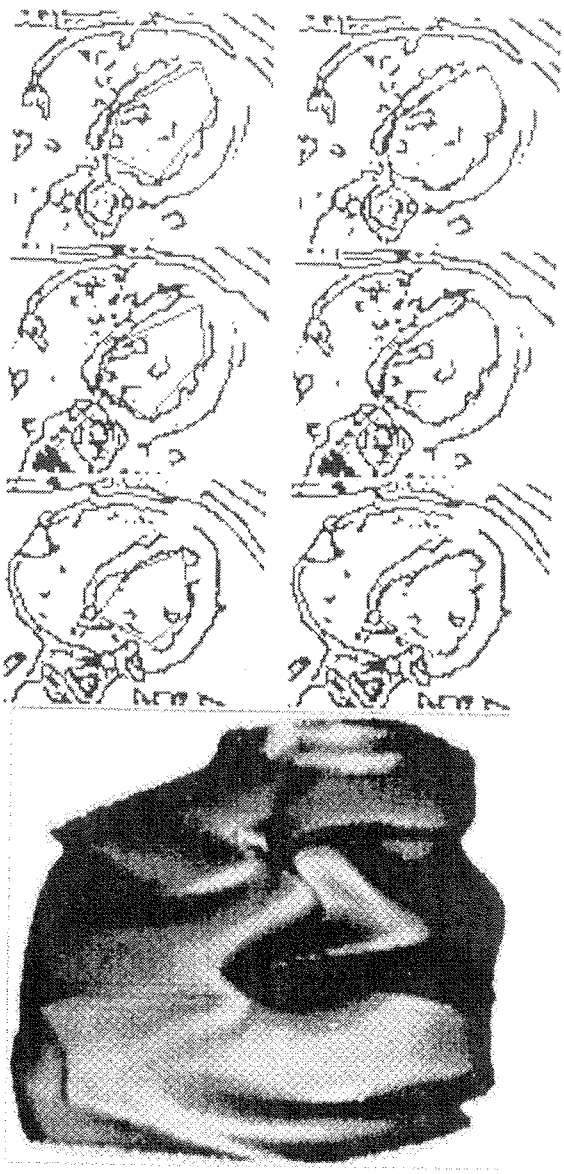

Figure 6: In this example we used a deformable surface constrained by boundary conditions (cylinder type) to segment the inside cavity of the left ventricle. We show the initial estimation superposed in light grey in some cross sections of the 3D image (1st column) and the final solution (2nd column). Bottom is the found 3-D representation of the inside cavity of the left ventricle. (Courtesy of I. Cohen and L. Cohen)

2.5 Geometric Tomography

In the same spirit as above, but for CTI, J.P. Thirion showed that it was possible to extract directly the boundary of contrasted objects from the edges of the sinograms (projections from which tomography is computed). The advantage is a much faster extraction of the edges directly from the data acquired by an X-Ray Scanner, without requiring the costly tomographic reconstruction itself. The method, called Geometric Tomography, has been patented by Inria [112]. It works particularly well with convex objects, as it is reported in [110].

2.6 Texture-Based Approaches

J. Lévy-Véhel, J.P. Berroir and P. Mignot [72], [74], and [73], implemented a system called ARTHUR which combines texture modelling and a sophisiticated discriminant analysis scheme to select a set of discriminant texture parameters from a training set of images (this approach has similarities with the work of [66]). The ARTHUR system can then be connected to a texture segmentation program called EXCALIBUR, which exploits the training phase and the notion of "mixed classes" to provide automatic segmentation of textured images. The texture operators include 2D and 3D texture operators, some of them involving advanced fractal and multifractal parameters.

3 Modeling Free-Form Surfaces

Once objects are segmented, they have to be modeled for further processing. This modeling is necessary for registration (next section), which is either rigid (some rigid part of a single patient) or deformable (nonrigid part of a single patient, inter-patient or patient-atlas registration). This a very challenging problem in medical image analysis, to study for instance the evolution of a pathology such as multiple sclerosis (MRI images), or the efficiency of a treatment against a cancer lesion (MRI or scanner images). This is also necessary to compare patients together and help therapy planification.

3.1 Extracting Ridges

The approach successfully developped in the Epidaure project consists in extracting typical lines, called ridges or crest lines, on the surface of the objects in each volumetric image.

Our definition of ridges on a surface is the locus of points where the maximum curvature (in absolute value) is extremal in the direction of maximum curvature. This definition does not apply when principal curvatures have the same absolute value, in particular at umbilics. Anyhow, as can be seen from experimental studies (see below) these ridges convey an intrinsic, meaningful and compact information on many anatomical surfaces:

- intrinsic, because ridge points are invariant with respect to rigid displacements (this comes from the intrinsic properties of the curvature).
- Meaningful, because ridges tend to correspond to anatomical features (this is the case on the face, the brain and the skull for instance as can be seen in figures 7, 10 and 9, and also in [26], [86], [87], [115], [60], [27]).
- Compact, because they represent a number of points typically 500 times more compact than the original image.

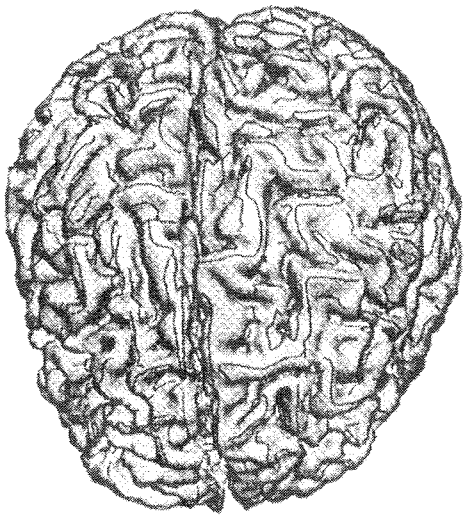

Figure 7: Ridges on the brain (Courtesy of J.P. Thirion and A. Gourdon)

Several definitions of ridge or crest lines can be found in [63], [33], [19] [98], [121], [40] and [90]. The one closer to our definition is probably in the book by Hosaka [57, page 98].

One should note that our definition of ridges is intrinsic to the isophote surface, without privileging any particular direction of the 3D space. One should refer to [64] for a rigorous and historical analysis of oriented ridges, i.e. ridges depending on a privileged direction in space.

Computing curvatures requires the extraction of the differential properties of the surfaces up to the 2nd order, while ridges require 3rd order differential properties. We show in the following subsections the different approaches we investigated to achieve a reliable ridge line extraction.

3.2 Local Fitting of Quadrics

After a segmentation of the 3D images, using for instance 3D edge detectors, O. Monga and P. Sander showed that it was then possible to use a local Kalman filter around each edgel, to fit a quadric surface in the least square sense. This polynomial approximation allows the computation of differential surface properties up to second order only (curvatures). This approach takes into account the uncertainty attached to the edge localisation and the surface normal, and provides an explicit estimation of the uncertainty attached to the computation of the principal curvatures. Unfortunately, although parallel in nature, the method is computationally very expensive. Curvature information is accurately extracted, but this is not the case for ridges [85].

3.3 Deriving the Image Intensity

Another approach is necessary to extract ridges. As we mentionned earlier, it is often a reasonable assumption to say that the boundary of an anatomical surface corresponds to an isophote (or iso-intensity) surface in

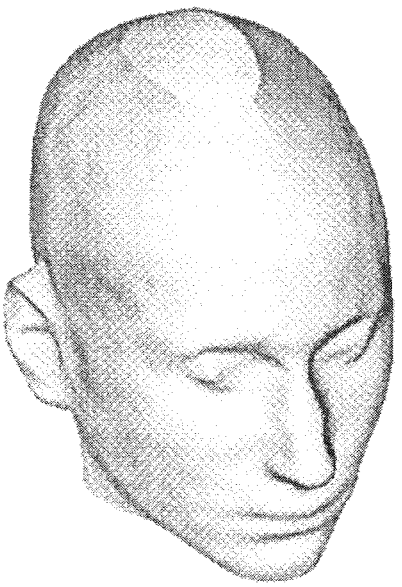

Figure 8: This figure shows the segmentation of a face with a deformable B-Spline within an image of the head acquired with MRI. Original MRI images were provided by Dr. Ericke, Siemens. (Courtesy of A. Guéziec).

Figure 9: This figure shows the ridges extracted from the previous B-Spline approximation. (Courtesy of A. Guéziec).

the volume image, especially with CTI but also with MRI and sometimes NMI. This assumption, combined with the implicit function theorem, allows the computation of the differential properties of the anatomical surface from the derivatives of the intensity function. This method provides excellent results in high resolution volumetric images, for a computational cost which can be maintained to a reasonable limit thanks to separable recursive filtering, as this is shown by O. Monga and S. Benayoun in [86] and [87], and by J.P. Thirion in [115].

Figure 7, shows the extraction of ridges on the brain surface acquired with MRI, while figure 10 shows the extraction of ridges on the surface of a skull acquired with CTI in 2 different positions.

The idea of deriving the intensity to extract different characteristic features, either on the intensity (hyper)surface or on isophote surfaces, is also successfully applied by (among others) [98], [121] and [90].

3.4 Using B-Spline Approximations

The previously mentionned deformable surfaces had 2 drawbacks: high computational complexity, and low-order derivability. The introduction of B-Splines with high order polynomials, thanks to their nice separability properties, reduces drastically these drawbacks while keeping the advantages of providing simultaneously a segmentation of anatomical surfaces and their local differential properties up to the third order for instance. This is very useful to track time-varying structures with rigid or nonrigid motion. The only limitation comes from the fact that the surface topology must be known in advance. This is described in details by A. Guéziec in [46], [48].

Figure 8 shows the segmentation of a face with a deformable B-Spline within an image of the head acquired with MRI, while figure 9 shows the extraction of ridges obtained from the B-Spline approximation.

3.5 The Marching Line Algorithm

In the 2 previous approaches (filtering and B-Splines), the connection of extracted ridge points to form ridges can be achieved by a very smart algorithm invented by J.P. Thirion, and called "the marching line algorithm". This algorithm looks for the zero-crossings of an extremality criterion (here the maximum curvature) in an isophote surface defined by a constant intensity level I. The algorithm insures both sub-voxel accuracy and nice topological properties like connectivity and closeness. Also, it can be applied simultaneously with the local filtering of isophote surfaces, to reduce drastically the filtering computing time if one seeks the extraction of major ridges only. A complete description of this algorithm can be found in [113], [115]. Ridges of figures 7, 9, and 10 were extracted with the marching line algorithm.

4 Rigid 3D Registration

I now describe with more details the problem of rigid 3D registration, because we believe it is a remarkable

illustration of computer vision applied to 3D medical images.

4.1 Importance of the Problem

As was mentionned before, a very common problem in medical image analysis is the automatic registration of 3D images of the same patient taken at different times, and in different positions. This is very useful to detect any pathological evolution, and to compute quantitative measurements of this evolution.

Performing this registration manually is a difficult task for a human operator, mainly because it requires quantitative spatial reasoning. The operator must discover corresponding anatomical landmarks, and locate them in 3D with a maximum accuracy. As the accuracy of the computed global registration increases with the number of matched correspondances, it is preferable to match as many landmarks as possible.Performing this task manually for tens of landmarks is extremely tedious, and it becomes definitely unfeasible with hundreds or thousands of landmarks.

Artificial landmarks could be used to simplify the point extraction and matching process. For instance a stereotaxic frame can be rigidly attached to the patient's skull. In fact, this is not a very confortable solution for the patient, and anyway such a frame cannot be worn during a long period (e.g. 6 months!). Moreover, it can happen that some displacement occurs between the frame and the patient between the 2 acquisitions, or that some internal organ moves with respect to the external frame (e.g. a sligth motion of the brain with respect to the skull). Finally, the accurate localization of specific points with artificial markers is usually not an obvious task.

For all these reasons, we believe that a fully automatic registration procedure relying only on detected anatomical landmarks is much more flexible and powerful than a manual procedure or than a procedure relying on artificial landmarks.

The output of the registration procedure must be the 6 independent parameters of the rigid displacement undergone by the region of interest between the 2 acquisitions. More precisely, one must compute the rotation and translation parameters which best match the two acquired images of this region of interest. At this point, it is important to note that because of potential occlusions, the two 3D images cannot be registered globally with a method based on the registration of the centers and axes of inertia.

4.2 Using Ridges and Geometric Hashing

The idea is to extract the maximum number of euclidean invariants computed exclusively on ridges and to use them for registration.

4.2.1 Euclidean Invariants on Surface Curves

We consider not only the curvature k and torsion τ of the ridge lines (the parameters which characterize completely a curve up to a rigid displacement), but also the maximum curvature of the surface, k_1, the angle θ between curve and surface normals and the angle ϕ between the curve tangent and the direction of the maximum curvature k_1 (see figures 16 and 17). These 5 intrinsic parameters are independent and allow for instance the computation of the second principal curvature of the surface through the computation of the normal curvature k_n, as well as the geodesic curvature k_g and torsion τ_g of the surface.

As the extraction of the ridge points required the computation of differential properties of the surface up to the 3rd order, the values of the maximum curvature value k_1 and direction e_1, as well as the surface normal N are readily available. But to compute the 5 intrinsic parameters $(k, \tau, k_1, \theta, \phi)$, we need to compute also the differential properties *of the curve itself* up to the 3rd order. A. Guéziec found that an efficient method was to approximate each ridge line (a discrete set of ridge points connected by the marching line algorithm) by a constrained B-Spline [47] (the B-Spline is constrained to have a tangent orthogonal to the surface normal). This provides a good estimation of the Frenet frame of the curve, (t, n, b), as well as the local curvature k and torsion τ. It is then immediate to compute $\theta = \text{angle}(n, N)$, and $\phi = \text{angle}\ (t, e_1)$.

4.2.2 Matching Algorithm

Once we know how to extract ridge points and how to compute the quantities $(k, \tau, k_1, \theta, \phi)$ at each ridge point, it is possible to design an extremely efficient matching algorithm. This algorithm, proposed by A. Guéziec, has 2 main stages, namely preprocessing and recognition, and combines geometric-hashing, accumulation, and prediction-verification [67], [6], [97], [2], [45], [119], [103], [37].

Preprocessing stage This stage can be applied off-line, a soon as the first image, called the model image, is acquired. The ridge lines are extracted from this image, and each ridge point with its Frenet frame (t, n, b) is stored in a 5 dimensional hash table based on the 5 intrinsic parameters $(k, \tau, k_1, \theta, \phi)$ attached to the ridge point.

The 5-dimension hash table is stored in a 1 dimensional array using classical but efficient hashing techniques.

Recognition stage Once the second image, called the scene image is acquired, it is necessary to apply the recognition stage on-line. The algorithm considers each ridge point S_i of the scene, and looks in the hash table for a model point with similar intrinsic parameters $(k, \tau, k_1, \theta, \phi)$. A difficult point is the notion of similarity, and a preliminary statistical study allowed for the definition of a statistical distance (Mahalanobis distance) based on the covariances of these parameters.

If a model point M_j is found with similar parameters in the hash table, the Frenet frames of both points are used to predict a rigid transformation T which maps both points with their Frenet frames. This transformation is accumulated in a 6 dimension accumulator of rigid transformations $\mathcal{A}$, by incrementing the cell whose coordinates correspond to T, and by keeping a pointer towards M_j and S_i. The uncertainty attached to the position of M_j and S_i is represented by 2 covariance matrices which are used to compute a covariance matrix Σ which represents the uncertainty on T.

When the accumulator cell already contains a rigid transformation T^- and a covariance Σ^-, both are up

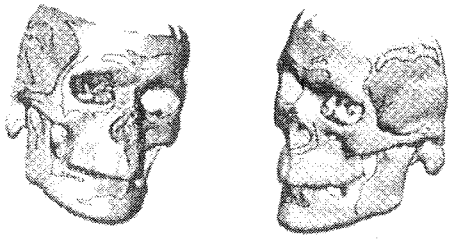

Figure 10: Top: Ridges (in black) extracted on the surface of a skull scanned in 2 different positions (left and right). Original 3D images are produced by a GE-CGR CT-Scan. (Courtesy of J.P. Thirion and A. Gourdon)

dated with a recursive least square procedure (the extended Kalman filter), and a new value T^+ is stored, with a new covariance matrix Σ^+ [2].

When all scene points have been treated, the algorithm looks for the accumulator cell which had the maximum number of access. This cell contains a transformation T^* with a covariance matrix Σ^*, and it is chosen as being the solution of the registration problem.

In the presented skull example, this transformation corresponds to the matching of 335 couples of ridge points. We can apply this transformation to all the ridge points of the model, and verify that they superimpose very nicely on the scene ridge points, as can be seen in figure 11. A quantitative analysis showed that the accuracy of the registration was better than one millimeter within the volume of the head [7].

4.2.3 Introduction of Extremal Points

J. P. Thirion introduced recently [111], [114] a new subset of intrinsic points he called "extremal points", which can be defined as the subset of ridge points for which the second principal curvature k_2 is also extremal in the associated direction e_2. These points have the nice property of being extrema of curvature of the 2 principal curvatures simultaneously, and can be defined as the intersection of 3 iso-surfaces: a chosen iso-intensity surface, and the two surfaces defined by the zero-crossings of the derivatives of k_i in the direction e_i for $i = 1, 2$. These derivatives can be computed everywhere but at points where the principal curvatures have identical absolute values, which includes again the umbilics..

Not only the extremal points have the property of being very stable and compact on anatomical surfaces (a few hundreds in a high resolution 3D image of the head), but some of them tend to be extremely stable from one patient to another one. They are therefore very good candidates as anatomical features for the Atlas Matching Problem described in a further section.

4.3 Matching a Cross Section with a 3D image

Another interesting problem is the matching of a cross-section with a 3D image. This happens when the patient must be registered with previously acquired 3D images during surgery for instance. In this case, only a

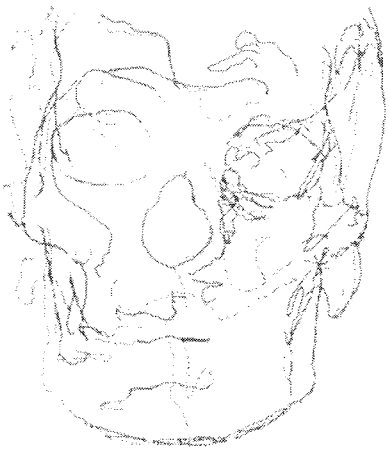

Figure 11: Automatic registration of the two sets of ridge lines (respectively solid and dotted lines), allowing a sub-voxel comparison of the 2 original 3D images. (Courtesy of A. Guéziec).

a few (possibly a single) cross-sections are acquired with a given modality, possibly with a laser range finder, and have to be matched with a surface extracted from a 3D image.

A. Gourdon showed that it was possible to exploit differential geometry constraints between the curve and the surface, to guide efficiently the correspondance algorithm. This is detailed in a forthcoming INRIA research report [44] and a typical result is shown in figure 12.

4.4 Matching with a Potential-Based Method

Computing ridges and euclidean invariants of second and third order requires high resolution images. This is currently not possible with NMI. Therefore, in this case, and in particular to combine together images of different modality like NMI and MRI for instance, other methods, usually based on potentials of attractions, can be used efficiently [78], [59], [117], [68], [14], [123]. Contrary to the method described in the previous section based on geometric hashing and euclidean invariants, potential-based methods require a preliminary estimation of the correct superposition, which might limit sometimes their robustness. Anyhow, excellent results can be obtained, as it is shown in figure 13 extracted from Malandain's and Rocchisani's work [78].

5 Deformations

Relaxing the rigidity assumption is necessary in two different problems, which are the atlas-matching problem and the analysis of nonrigid motion.

5.1 The Atlas Matching Problem

Building an "electronic atlas" of the human body is again a very challenging issue for the future, and several teams have contributed to this topic. Among them, one

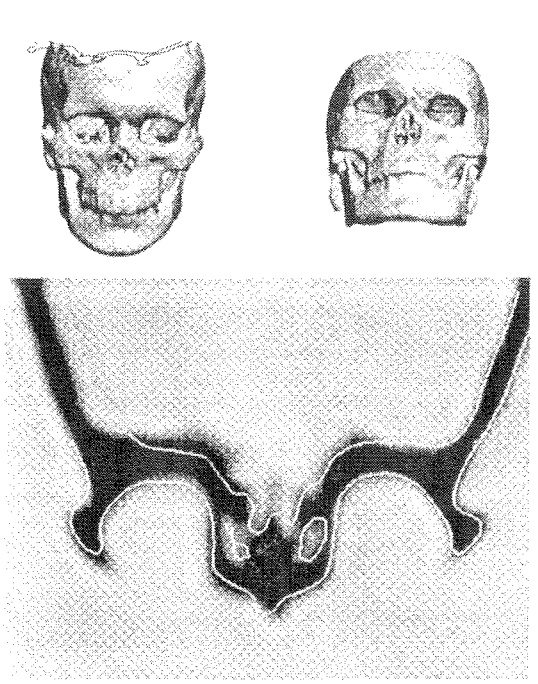

Figure 12: Left: a surface is extacted from a 3D CTI image and a curve is extracted from another 2D cross section. Right: the curve is matched on the surface, with the use of differential geometry constraints. Bottom: superposition of the curve in the image plane extracted from the 3D image. (Courtesy of A. Gourdon).

must aknowledge the pioneering work of [8] more than 10 years ago!

Some recent work, like the one of [55] is more oriented towards the construction of a visualization database. Our goal is oriented towards the automatic registration of such an atlas against the 3D image of an arbitrary patient. For doing this, we believe that ridge lines are good anatomical invariants, and can therefore serve as a sound geometrical basis to build a computerized anatomical atlas of some parts of the human body. This assumption is supported by our experimental studies, and by statistical and anthropological studies [27], [60].

Having built a "generic model", the problem is then to find a matching algorithm which can register it with the 3D image of an arbitrary patient. Such an algorithm could also help making inter-patient registrations, and comparisons.

The current strategy within the Epidaure project, is to define a constrained network of ridge lines and extremal points [105], [111], [114], which could deform itself to adapt to the geometry of a given patient. The spirit is similar to the one introduced by [122]. Having matched this subset of characteristic lines and points, it should be possible to obtain registration everywhere, by applying for instance a constrained interpolation with B-splines [17], [16], [28].

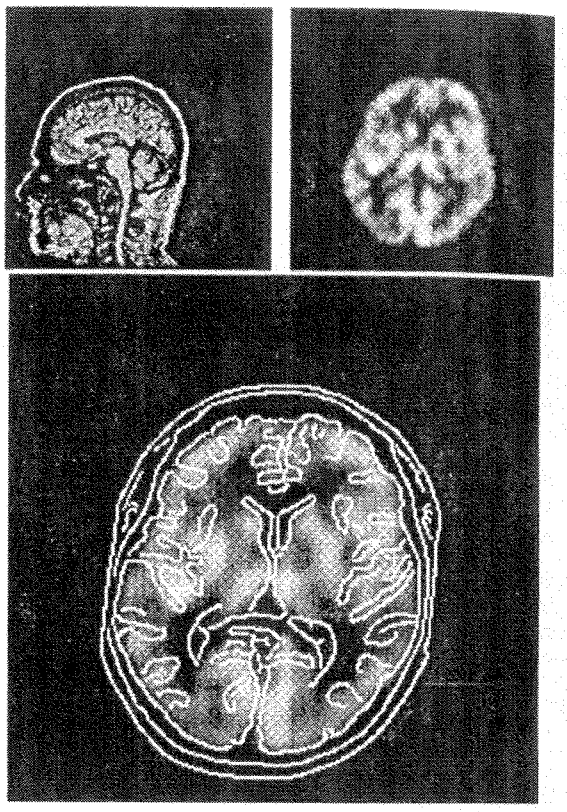

Figure 13: A potential based method allows the registration of an MRI image (top left) with a NMI image of the head (top right). Interpolated cross section of the registered 3D MRI is computed, and its edges are shown superimposed on the NMI images (bottom). Images are courtesy of Jael Travere, from the Cyceron Center in Caen, France. (Courtesy of G. Malandain and J.M. Rocchisani).

The ideas of [24], who take advantage of a principal components analysis of a training data set to constrain the deformation of the model, could certainly be applied fruitfully.

We show in figure 18 a preliminary result of the matching of a skull atlas on a 3D CT image of a patient.

5.2 Analyzing nonrigid motion

In time sequences of 3D images, like USI, MRI or NMI images of the beating heart, it would be extremely profitable not only to track the motion of moving structures, but also to provide the physicians with a reduced set of pertinent parameters which describe their nonrigid motion. Usually, the problem is dual: first it is necessary to find the motion of individual points, then it is necessary to approximate this motion with a reduced number of parameters.

5.2.1 Motion of Individual Points

Tracking structures with deformable models like snakes usually does not provide the motion of each individual point, but only a global registration of a curve (or surface) against a curve (or surface). A post-processing, which takes into account the presence of geometric singularities along the tracked structures, and in particular curvature singularities, can be used to find point to point correspondences [21], [12], [34], [1], [83] [38], [99].

Good results can also be obtained with a physically-based deformable model which provides tracking and point-to-point correspondences at the same time [92], [109]. Figure 14 shows the use of the deformable model of C. Nastar to track the mitral valve in images of the heart acquired with USI, and get point to point correspondances.

5.2.2 Global Analysis of motion

Once point-to-point correspondances have been established, it is possible to project on a reduced basis the set of displacements. This is the purpose of modal analysis, where the basis corresponds to a reduced set of some "qualitative" deformations [56], [95], or to the major monofrequency vibration harmonics of the elastic structure [92].

A major advantage of the latest approach is the possibility to compute analytically [91] the modes beforehand, which reduces tremendously the computational complexity. Figure 15 shows a modal approximation of the 2D motion of the mitral valve shown in figure 14.

Global analysis of nonrigid motion can also be obtained with parametrable deformable shapes using for instance superquadrics [10], [107], [82], [118] or Fourier models [102].

6 Surgery Simulation

A fascinating new field, at the intersection of computer vision, computer graphics, and robotics, is the exploitation of 3D images to planify, simulate, and even control some complex therapy (e.g. [94],[69], [9]). Among them, cranofacial surgery or laparoscopy for instance, are desperatly seeking for pre-operative simulation [26], [79]. This can be done with the help of pre-operative 3D image analysis, and the use of advanced interactive 3D graphics involving virtual reality for instance [93], [39], [62].

Currently, in the Epidaure project, H. Delingette and G. Subsol, with the help of S. Cotin and J. Pignon [31], [30] are looking closely at the problem of simulating cranio-facial surgery, following the ideas of the pioneering work of Terzopoulos and Waters [109]. This is illustrated by figure 19.

Another related impressive work is the simulation of birth delivery, studied by B. Geiger and J.D. Boissonnat within the Prisme project at Inria [41], [15].

7 Conclusion

I tried to show in this paper that automating the analysis of 3D medical images was an abundant field of new research topics in computer vision and robotics. I presented the past and current work of the research group EPIDAURE at INRIA, and tried to define current trends and future challenges for research.

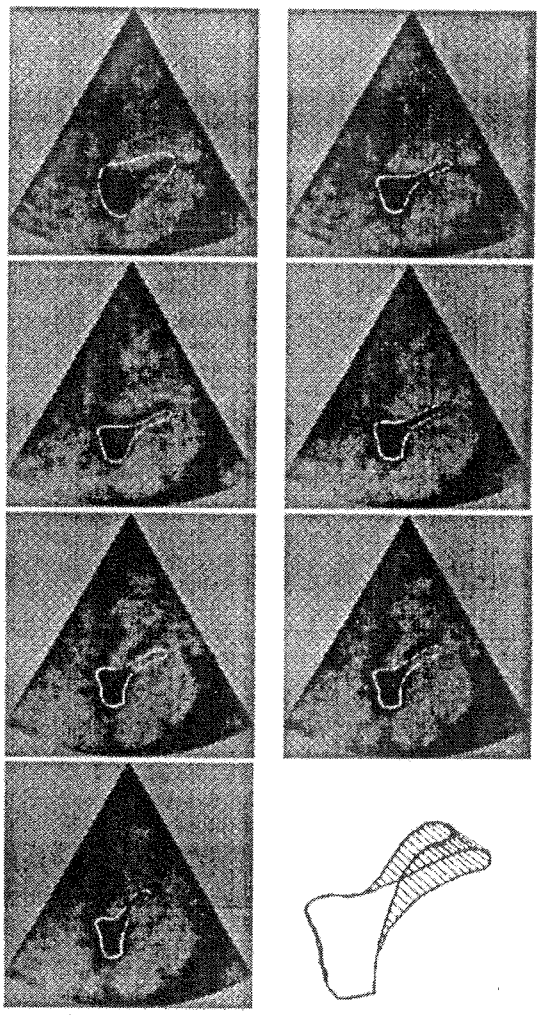

Figure 14: From left to right and top to bottom: (a)(b) Segmentation and (c-g) tracking of the mitral valve of the heart in a sequence of USI using the active physical model of C. Nastar. (g) shows the obtained point to point correspondances. These images were preprocessed with the sonar-space filtering method of I. Herlin referenced in the text. (Courtesy of C. Nastar).

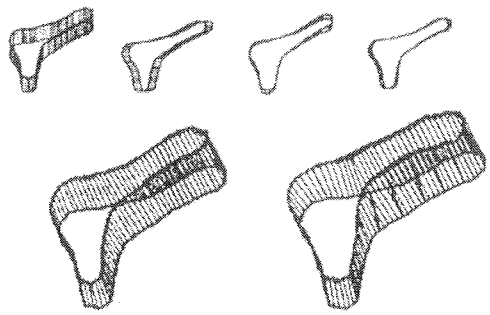

Figure 15: From left to right and top to bottom: four high amplitude eigenmodes of the valve (a,b,c,d). Their superposition (e) compared to the expected result (f). (Courtesy of C. Nastar).

One of these challenges will be the capability of transferring the knowledge from the research centers to the hospitals. This will require the creation of a number of companies starting selling dedicated software and hardware.

J. Engelberger [36] made the prediction in 1988 that the new big market for robotics was the domestic robot, and his prediction was including medical robotics. I feel that a potentially enormous new market for computer vision itself is going to be 3D medical image processing.

8 Acknowledments

Of course, aknowledments go primarily to the researchers of the EPIDAURE group who actively contributed during the past 4 years to the research work presented in this paper. They are, by alphabetical order, **I. Cohen, L. Cohen, A. Guéziec, I. Herlin, J. Lévy-Véhel, G. Malandain, O. Monga, J.M. Rocchisani, and J.P. Thirion**. More recently, important contributions also came from **E. Bardinet, S. Benayoun, J.P. Berroir, H. Delingette, J. Feldmar, A. Gourdon, P. Mignot, C. Nastar and G. Subsol**. This work benefited from close interactions with **R. Hummel** during a one year sabbatical he spent in our group, and also with **J.D. Boissonnat, P. Cinquin, C. Cutting, R. Kikinis, O. Kubler, B. Geiger, D. Geiger and J. Travere**. Thanks also to our system engineer, **J.P. Chièze** who made everything work!

Digital Equipement supported a significant part of this research and **GE-CGR** in Buc, France, supported part of the rigid matching research work. **Matra-MS2I** and **Philips** supported part of the research on ultrasound images. **Aleph-Med** and **Focus-Med** in Grenoble contribute to the transfer of software towards industry. The European project **AIM-Murim** supported collaborations with several European imaging and robotics. Finally the Esprit European project called **BRA-VIVA** supported part of the work on the extraction and use of euclidean invariants for matching.

Many thanks to **S. Dewez**, **A. Eidelman**, and **B. Hidoine**, from the Video Department of Inria, for their help in producing iconic representations of our results, and in particular the movie called "In Man's Image".

References

[1] A. Amini, R. Owen, L. Staib, P. Anandan, and J. Duncan. Non-rigid motion models for tracking the left ventricular wall. In A. Colchester and D. Hawkes, editors, *Information Processing in Medical Imaging, IPMI'91*, Lecture notes in computer science. Springer-Verlag, 1991.

[2] N. Ayache. *Artificial Vision for Mobile Robots: Stereovision and Multisensor Perception*. MIT-Press, 1991.

[3] N. Ayache, J.D. Boissonnat, L. Cohen, B. Geiger, J. Levy-Vehel, O. Monga, and P. Sander. Steps toward the automatic interpretation of 3D images. In K. Hohne, H. Fuchs, and S. Pizer, editors, *3D imaging in medicine*, pages 107–120. Springer Verlag, 1990. NATO ASI Series, Vol. F60.

[4] N. Ayache, P. Cinquin, I. Cohen, L. Cohen, F. Leitner, and O. Monga. Segmentation of complex 3D medical objects: a challenge and a requirement for computer assisted surgery planning and performing. In R. Taylor and S. Lavallee, editors, *Computer Integrated Surgery*. MIT Press, 1994. in press.

[5] N. Ayache, I. Cohen, and I. Herlin. Medical image tracking. In A. Blake and A. Yuille, editors, *Active Vision*, chapter 17. MIT-Press, 1992.

[6] N. Ayache and O.D. Faugeras. Hyper: A new approach for the recognition and positioning of two-dimensional objects. *IEEE Transactions on Pattern Analysis and Machine Intelligence*, 8(1):44–54, January 1986.

[7] N. Ayache, A. Gueziec, J.P. Thirion, A. Gourdon, and J. Knoplioch. Evaluating 3D registration of ct-scan images using crest lines. In *Mathematical methods in medical images*, San-Diego, USA, July 1993. Spie-2035-03.

[8] Ruzena Bajcsy, Robert Lieberson, and Martin Reivich. A computerized system for the elastic matching of deformed radiographic images to idealized atlas images. *Journal of Computer Assisted Tomography*, 7(4):618–625, 1983.

[9] H. Baker, J. Bruckner, and J. Langdon. Estimating ankle rotational constraints from anatomic structure. In R. Robb, editor, *Visualization in Biomedical Computing*, volume 1808, pages 422–432. SPIE, 1992. Chapell Hill.

[10] E. Bardinet, N. Ayache, and L. Cohen. Non-rigid 3D motion analysis using superquadrics. *INRIA research report*, September 1993. in preparation.

[11] H. Barrett and A. Gmitro, editors. *Int. Conf. on Information Processing in Medical Images, IPMI'93*, Flagstaff, Usa, 1993. Springer Verlag. Lecture Notes in Computer Science, No 687.

[12] S. Benayoun and N. Ayache. 3D motion analysis using differential geometry constraints. *INRIA research report*, September 1993. in preparation.

[13] G. Bertrand and G. Malandain. A new characterization of three-dimensional simple points. *Pattern Recognition Letters*, 1993. Accepted for publication.

[14] P.J. Besl and McKay N.D. A method for registration of 3D shapes. *IEEE Transactions on PAMI*, 14:239–256, February 1992.

[15] J-D. Boissonnat and B. Geiger. 3D reconstruction of complex shapes based on the delaunay triangulation. *Inria research report*, (1697), 1992.

[16] Fred L. Bookstein. Principal warps: Thin-plate splines and the decomposition of deformations. *IEEE Transactions on Pattern Analysis and Machine Intelligence*, 11(6):567–585, June 1989.

[17] Fred L. Bookstein and William D.K. Green. Edge information at landmarks in medical images. In *Visualization in Biomedical Computing 1992*, pages 242–258. SPIE, 1992.

[18] M. Brady and S. Lee. Visual monitoring of glaucoma. *Image and Vision Computing*, 9(4):39–44, 1991.

[19] Michael Brady, Jean Ponce, Alan Yuille, and Haruo Asada. Describing surfaces. In Hideo Hanafusa and Hirochika Inoue, editors, *Proceedings of the Second International Symposium on Robotics Research*, pages 5–16, Cambridge, Mass., 1985. MIT Press.

[20] I. Cohen, L. D. Cohen, and N. Ayache. Using deformable surfaces to segment 3-D images and infer differential structures. *Computer Vision, Graphics and Image Processing: Image Understanding*, 56(2):242–263, 1992.

[21] Isaac Cohen, N. Ayache, and P. Sulger. Tracking points on deformable curves. In *Proceedings of the Second European Conference on Computer Vision 1992*. Santa Margherita Ligure, Italy, May 1992.

[22] L. D. Cohen. On active contour models and balloons. *Computer Vision, Graphics and Image Processing: Image Understanding*, 53(2):211–218, March 1991.

[23] L. D. Cohen and I. Cohen. Finite element methods for active contour models and balloons for 2-D and 3-D images. *IEEE Transactions on Pattern Analysis and Machine Intelligence*, 1993. In press.

[24] T.F. Cootes, A. Hill, C.J. Taylor, and J. Haslam. The use of active shape models for locating structures in medical images. In H.H. Barrett and A.F. Gmitro, editors, *Information Processing in Medical Imaging*, pages 33–47, Flagstaff, Arizona (USA), June 1993. IPMI'93, Springer-Verlag.

[25] R. Curwen and A. Blake. Dynamic contours: real time active splines. In A. Blake and A. Yuille, editors, *Active Vision*, chapter 3. MIT-Press, 1992.

[26] C. Cutting. Applications of computer graphics to the evaluation and treatment of major craniofacial malformations. In J. Udupa and G. Herman, editors, *3D imaging in medicine*, chapter 6, pages 163–189. CRC-Press, 1991.

[27] C. Cutting, F. Bookstein, B. Haddad, D. Dean, and D. Kim. A spline based approach for averaging 3D curves and surfaces. In *Mathematical methods in medical images*, San-Diego, USA, July 1993. Spie-2035-03.

[28] J. Declerck and J.P. Thirion. Constrained B-Splines for approximating 3D anatomical structures. Technical report, INRIA, 1993. in preparation.

[29] H. Delingette, M. Hebert, and K. Ikeuchi. Shape representation and image segmentation using deformable surfaces. *Image and Vision Computing*, 10(3):132–144, April 1992.

[30] H. Delingette, G. Subsol, J. Pignon, and S. Cotin. Application of simplex mesh to cranio-facial surgery. Technical report, I.N.R.I.A., Septembre 1993. in preparation.

[31] H. Delingette, Y. Watanabe, and Y. Suenaga. Simplex based animation. In N. Magnenat-Thalmann and D. Thalmann, editors, *Models and Techniques in Computer Animation*, pages 13–28, Geneva (Switzerland), June 1993. Computer Animation, Springer Verlag.

[32] R. Deriche. Using canny's criteria to derive a recursively implemented optimal edge detector. *International Journal of Computer Vision*, 1(2), May 1987.

[33] Manfredo P. do Carmo. *Differential Geometry of Curves and Surfaces*. Prentice-Hall, Englewood Cliffs, 1976.

[34] J.S. Duncan, R.L. Owen, L.H. Staib, and P. Anandan. Measurement of non-rigid motion using contour shape descriptors. In *Proc. Computer Vision and Pattern Recognition*, pages 318–324, Lahaina, Maui, Hawaii, June 1991.

[35] Les Echos, 5 December 1991. in French.

[36] J. Engelberger. Domesticating the industrial robot. In R. Jarvis, editor, *Int. Symposium on Industrial Robots*, pages 21–39, Sydney, Australia, 1988. ISIR'88. Springer-Verlag.

[37] O. Faugeras. *3D computer vision, a geometric viewpoint*. MIT-Press, 1993.

[38] D. Friboulet, I. Magnin, A. Pommert, and M. Amiel. 3D curvature features of the left ventricle from CT volumic images. In *SPIE, Mathematical Methods in Medical Imaging*, volume 1768, pages 182–192, July 1992, San Diego.

[39] H. Fuchs. Systems for display of 3D medical image data. In K. Hohne, H. Fuchs, and S. Pizer, editors, *3D imaging in medicine*, pages 315–331. Springer Verlag, 1990. NATO ASI Series, Vol. F60.

[40] J. Ganch and S. Pizer. Multiresolution analysis of ridges and valleys in grey scale images. *IEEE Transactions on Pattern Analysis and Machine Intelligence*, 15(6):635–646, 1993.

[41] B. Geiger. 3D simulation of delivery for cephalopelvic disproportion. In *First int. works. on mechatronics in medicine and surgery*, October 1992. Costa del Sol.

[42] D. Geiger and J. Vlontzos. Dynamic programming for detecting tracking and matching deformable contours, 1993.

[43] G. Gerig, W. Kuoni, R. Kikinis, and O. Kubler. Medical imaging and computer vision: an integrated approach for diagnosis and planning. In H. Burkhardt, K. Hohne, and B. Neumann, editors, *Proc. 11. DAGM symposium*, volume 219, pages 425–432, Sydney, Australia, 1989. Springer-Verlag. Informatik Fachberichte.

[44] A. Gourdon and Ayache N. Matching a curve on a surface using differential properties, 1993.

[45] E. Grimson. *Object Recognition by Computer*. MIT-Press, 1991.

[46] A. Gueziec. Large deformable splines, crest lines and matching. In *Int. Conf. on Computer Vision, ICCV'93*, Berlin, Germany, 1993.

[47] A. Guéziec and N. Ayache. Smoothing and matching of 3–D-space curves. In *Proceedings of the Second European Conference on Computer Vision 1992*, Santa Margherita Ligure, Italy, May 1992. to be published in the Int. J. of Computer Vision in 1993.

[48] A. Guéziec and N. Ayache. Large deformable splines, crest lines and matching. In *Geometric methods in computer vision'93*, San-Diego, USA, July 1993. Spie-2035-03.

[49] C. Harris. Tracking with rigid models. In A. Blake and A. Yuille, editors, *Active Vision*, chapter 4. MIT-Press, 1992.

[50] I.L. Herlin and N. Ayache. Features extraction and analysis methods for sequences of ultrasound images. *Image and Vision Computing*, 10(10):673–682, December 1992.

[51] I.L. Herlin and N. Ayache. Features extraction and analysis methods for sequences of ultrasound images. In *Proceedings of the Second European Conference on Computer Vision 1992*, Santa Margherita Ligure, Italy, May 1992.

[52] I.L. Herlin, C. Nguyen, and Ch. Graffigne. A deformable region model using stochastic processes applied to echocardiographic images. In *Proc. Computer Vision and Pattern Recognition*, Champaign, Illinois, U.S.A., 15-18 June 1992.

[53] G.T. Herman. Discrete multidimensional jordan surfaces. *Computer Vision, Graphics, and Image Processing: Graphical Models and Image Processing*, 54(6):507–515, november 1992.

[54] K. Hohne, H. Fuchs, and S. Pizer, editors. *3D imaging in medicine*. Springer Verlag, 1990. NATO ASI Series, Vol. F60.

[55] K. Hohne, A. Pommert, M Riemer, T. Schiemann, R. Schubert, and U. Tiede. Framework for the generation of 3D anatomical atlases. In R. Robb, editor, *Visualization in Biomedical Computing*, volume 1808, pages 510–520. SPIE, 1992. Chapell Hill.

[56] B. Horowitz and A. Pentland. Recovery of non–rigid motion and structure. In *Proc. Computer Vision and Pattern Recognition*, pages 325–330, Lahaina, Maui, Hawaii, June 1991.

[57] M. Hosaka. *Modeling of Curves and Surfaces in CAD/CAM*. Springer Verlag, 1992.

[58] F. Hottier and A. Collet-Billon. 3D echography: Status and perspective. In K. Hohne, H. Fuchs, and S. Pizer, editors, *3D imaging in medicine*, pages 21–41. Springer Verlag, 1990. NATO ASI Series, Vol. F60.

[59] H. Jiang, R. Robb, and K. Holton. a new approach to 3D registration of multimodality medical images by surface matching. In R. Robb, editor, *Visualization in Biomedical Computing*, volume 1808, pages 196–213. SPIE, 1992. Chapell Hill.

[60] A. Kalvin, D. Dean, J. Hublin, and M. Braun. Visualisation in anthropology: reconstruction of human fossils from multiple pieces. In A. Kaufman and G. Nielson, editors, *Proc. of the IEEE Visualization'92*, pages 404–410. 1992.

[61] Michael Kass, Andrew Witkin, and Demetri Terzopoulos. Snakes: Active contour models. *International Journal of Computer Vision*, 1:321–331, 1987.

[62] R. Kikinis, H. Cline, D. Altobelli, M. Halle, W. Lorensen, and F. Jolesz. Interactive visualisation and manipulation of 3D reconstructions for the planning of surgical procedures. In R. Robb, editor, *Visualization in Biomedical Computing*, volume 1808, pages 559–563. SPIE, 1992. Chapell Hill.

[63] J. Koenderink. *Solid Shape*. MIT-Press, 1990.

[64] J. Koenderink. local features of smooth shapes: ridges and courses. In *SPIE, Geometric Methods in Computer Vision II*, pages 2–13, 1993. San Diego.

[65] T.Y. Kong and A. Rosenfeld. Digital topology: introduction and survey. *Computer Vision, Graphics, and Image Processing*, 48:357–393, 1989.

[66] O. Kubler and G. Gerig. Segmentation and analysis of multidimensional data sets in medicine. In K. Hohne, H. Fuchs, and S. Pizer, editors, *3D imaging in medicine*, pages 63–81. Springer Verlag, 1990. NATO ASI Series, Vol. F60.

[67] Y. Lamdan and H. Wolfson. Geometric hashing: a general and efficient model-based recognition scheme. In *Proceedings of the Second International Conference on Computer Vision (ICCV)*, 1988.

[68] S. Lavallée, R. Szeliski, and L. Brunie. Matching 3D smooth surfaces with their 2d projections using 3D distance maps. In *SPIE, Geometric Methods in Computer Vision*, July 25–26 1991. San Diego.

[69] S. Lavallee, J. Troccaz, L. Gaborit, P. Cinquin, A.L Benabid, and D. Hoffmann. Image ginded robot: a clinical application in stereotactic neurosurgery. In *IEEE int. conf. on robotics and automation*, pages 618–625, 1992. Nice, France.

[70] Simon Lee. *Visual Monitoring of Glaucoma*. PhD thesis, Robotics Research Group, Department of Engineering Science, University of Oxford, 1991.

[71] S. Leitner, I. Marque, S. Lavallee, and P. Cinquin. Dynamic segmentation: finding the edge with spline snakes. In P.J. L., A. Le Mehaute, and L.L. Schumaker, editors, *Curves and Surfaces*, pages 279–284. Academic Press, 1991.

[72] J. Levy-Vehel. Texture analysis using fractal probability functions. *INRIA research report*, (1707), 1993.

[73] J. Levy-Vehel, P. Mignot, and J.P. Berroir. Multifractal, texture and image analysis. In *CVPR'92*, Urbana Champaign, 1992.

[74] J. Levy-Vehel, P. Mignot, and J.P. Berroir. Texture and multifractals : New tools for image analysis. *INRIA research report*, (1706), 1993.

[75] F. Leymarie and M. Levine. Tracking deformable objects in the plane using an active contour model. *IEEE Transactions on Pattern Analysis and Machine Intelligence*, 15(6):635–646, 1993.

[76] H. Maitre and F. Preteux. Progress in digital image processing with applications to medical imaging, 1993. ENST Internal report, 46 rue barrault, 75013 Paris. France.

[77] G. Malandain, G. Bertrand, and N. Ayache. Topological segmentation of discrete surfaces. *International Journal of Computer Vision*, 10(2):183–197, 1993.

[78] G. Malandain and J.M. Rocchisani. Registration of 3D medical images using a mechanical based method. In *IEEE EMBS satellite symposium on 3D advanced image processing in medicine*, November 2–4 1992. Rennes, France.

[79] D. Marchac and D. Renier. New aspects of crano-facial surgery. *World Journal of Surgery*, 14:725–732, July 1990.

[80] T. McInerney and D. Terzopoulos. A finite element model for 3D shape reconstruction and nonrigid motion tracking. In *Int. Conf. on Computer Vision, ICCV'93*, pages 518–523, Berlin, Germany, 1993.

[81] S. Menet, P. Saint-Marc, and G. Medioni. Active contour models: Overview, implementation and applications. *System, Man and Cybernetics*, pages 194–199, 1993.

[82] D. Metaxas and D. Terzopoulos. Shape and nonrigid motion estimation through physics-based synthesis. *IEEE Transactions on Pattern Analysis and Machine Intelligence*, 15(6):580–591, 1993.

[83] Sanjoy K. Mishra, Dmitry B. Goldgof, and Thomas S. Huang. Motion analysis and epicardial deformation estimation from angiography data. In *Proc. Computer Vision and Pattern Recognition*, pages 331–336. IEEE Computer Society Conference, June 1991. Lahaina, Maui, Hawaii.

[84] Le Monde, 6 April 1993. page 27. in French.

[85] O. Monga, N. Ayache, and P. Sander. Using uncertainty to link edge detection and local surface modelling. *Image and Vision Computing*, 10(6):673–682, 1992.

[86] O. Monga, S. Benayoun, and O. Faugeras. From partial derivatives of 3D density images to ridge lines. In M. Robb, editor, *Visualisation in Biomedical computing, VBC'92*, pages 118–129. Chapel Hill, Usa, 1992. Spie vol. 1808.

[87] O. Monga, S. Benayoun, and O. Faugeras. From partial derivatives of 3D volumetric images to ridge lines. In *IEEE Conf. on Computer Vision and Pattern Recognition, CVPR'92*, Urbana Champaign, 1992.

[88] O. Monga, R. Deriche, G. Malandain, and J.P. Cocquerez. Recursive filtering and edge closing: 2 primary tools for 3D edge detection. *Image and Vision Computing*, 9(4), august 1991.

[89] O. Monga, R. Deriche, and JM. Rocchisani. 3D edge detection using recursive filtering. *Computer Vision, Graphics and Image Processing*, 53(1), january 1991.

[90] B. Morse, S. Pizer, and A. Liu. Multiscale medial analysis of medical images. In H.H. Barrett and A.F. Gmitro, editors, *Information Processing in Medical Imaging*, pages 112–131, Flagstaff, Arizona (USA), June 1993. IPMI'93, Springer-Verlag.

[91] C. Nastar. Analytical computation of the free vibration modes : Application to non rigid motion analysis and animation in 3D images. Technical Report 1935, INRIA, June 1993.

[92] C. Nastar and N. Ayache. Fast segmentation, tracking, and analysis of deformable objects. In *Proceedings of the Fourth International Conference on Computer Vision (ICCV 93)*, Berlin, May 1993. also in SPIE, Geometric Methods in Computer Vision, San-Diego, 1993.

[93] R. Ohbuchi, D. Chen, and H. Fuchs. Incremental volume reconstruction and rendering for 3D ultrasound imaging. In R. Robb, editor, *Visualization in Biomedical Computing*, volume 1808, pages 312–323. SPIE, 1992. Chapell Hill.

[94] H. Paul, B. Mittlestadt, W. Bargar, B. Musits, Russ Taylor, P. Kazanzides, J. Zuhars, B. Williamson, and W. Hanson. A surgical robot for total hip replacement surgery. In *IEEE int. conf. on robotics and automation*, pages 606–611, 1992. Nice, France.

[95] Alex Pentland and Stan Sclaroff. Closed-form solutions for physically based shape modelling and recognition. *IEEE Transactions on Pattern Analysis and Machine Intelligence*, 13(7):715–729, July 1991.

[96] S. Pizer, editor. *Visualisation in Biomedical computing, VBC'92*, Chapel Hill, Usa, 1992. Spie vol. 1808.

[97] I. Rigoutsos and R. Hummel. Implementation of geometric hashing on the connection machine. In *Proceedings of the IEEE Workshop on directions of automated cad-based vision*, 1991.

[98] B. Harr Romeny, L. Florack, A. Salden, and M. Viergever. Higher order differential structure of images. In H.H. Barrett and A.F. Gmitro, editors, *Information Processing in Medical Imaging*, pages 77–93. Flagstaff, Arizona (USA), June 1993. IPMI'93, Springer-Verlag.

[99] N. Rougon. On mathematical foundations of local deformations analysis. In *Mathematical methods in medical imaging II*, volume 2035, San-Diego, USA, July 1993. Spie.

[100] Science et Technologie, February 1991. Special Issue on Medical Images, in French.

[101] J. Serra. *Image Analysis and Mathematical Morphology*. Academic Press, 1982.

[102] L. Staib and J. Duncan. Deformable fourier models for surface finding in 3D images. In R. Robb, editor, *Visualization in Biomedical Computing*, volume 1808, pages 90–104. SPIE, 1992. Chapell Hill.

[103] F. Stein. Structural hashing: efficient 3D object recognition. In *Proc. Computer Vision and Pattern Recognition*, Lahaina, Maui, Hawaii, June 1991.

[104] M Stytz, G Frieder, and O. Frieder. Three-dimensional medical imaging: algorithms and computer systems. *ACM Computer Surveys*, 23(4):421–499, December 1991.

[105] G. Subsol, J.P.Thirion, and N. Ayache. Recognition of generic models with networks of active lines. Technical report, INRIA, 1993. in preparation.

[106] D. Terzopoulos, A.Witkin, and M. Kass. Symmetry seeking models for 3D object reconstruction: Active contour models. In *Proceedings of the first International Conference on Computer Vision (ICCV 87)*. London, June 1987.

[107] D. Terzopoulos and D. Metaxas. Dynamic 3-D models with local and global deformations: Deformable superquadrics. *IEEE Transactions on Pattern Analysis and Machine Intelligence*, 13(7):703–714, 1991.

[108] D. Terzopoulos and R. Szeliski. Tracking with Kalman snakes. In A. Blake and A. Yuille, editors, *Active Vision*, chapter 1. MIT-Press, 1992.

[109] D. Terzopoulos and K. Waters. Analysis and synthesis of facial image sequences using physical and anatomical models. *IEEE Transactions on Pattern Analysis and Machine Intelligence*, 15(6):569–579, 1993.

[110] J-P Thirion. Segmentation of tomographic data without image reconstruction. *IEEE Trans. on Medical Imaging*, 11(1):102–110, March 1992.

[111] J-P. Thirion. New feature points based on geometric invariants for 3D image registration. *INRIA research report*, (1901), April 1993.

[112] J-P. Thirion and N. Ayache. Procédé et dispositif d'aide à l'inspection d'un corps, notamment pour la tomographie. Brevet Français, numero 91 05138, Avril 1991. En cours d'extension internationale (numero 92 00252).

[113] J-P. Thirion, N. Ayache, O. Monga, and A. Gourdon. Dispositif de traitement d'informations d'images tri-dimensionnelles avec extraction de lignes remarquables. Brevet Français, numero 92 03900, Mars 1992. Pattent pending.

[114] J-P. Thirion and S. Benayoun. Image surface extremal points, new feature points for image registration. *INRIA research report*, September 1993. in preparation.

[115] J-P. Thirion and A. Gourdon. The 3D marching lines algorithm : new results and proofs. *INRIA research report*, (1881), March 1993.

[116] J. Udupa and G. Herman, editors. *3D imaging in medicine*. CRC-Press, 1991.

[117] P. van den Elsen, A. Maintz, E. Pol, and M. Viergever. Image fusion using geometrical features. In M. Robb, editor, *Visualisation in Biomedical computing, VBC'92*, pages 172–186, Chapel Hill, Usa, 1992. Spie vol. 1808.

[118] B. Vemuri, A. Radisavljevic, and C. Leonard. Multiresolution stochastic 3D shape models for image segmentation. In H.H. Barrett and A.F. Gmitro, editors, *Information Processing in Medical Imaging*, pages 62–76, Flagstaff, Arizona (USA), June 1993. IPMI'93, Springer-Verlag.

[119] W.M. Wells III. Posterior Marginal Pose Estimation. In *Proceedings: Image Understanding Workshop*, pages 745 – 751. Morgan Kaufmann, January 1992.

[120] W.M. Wells III, E. Grimson, T. Kanade, and N. Ayache, editors. *Applications of Computer Vision in Medical Image Processing*. AAAI Workshop, May 1994. Stanford.

[121] R. Whitaker. Characterizing first and second-order patches using geometry limited diffusion. In H.H. Barrett and A.F. Gmitro, editors, *Information Processing in Medical Imaging*, pages 149–167, Flagstaff, Arizona (USA), June 1993. IPMI'93, Springer-Verlag.

[122] Alan L. Yuille, Peter W. Hallinan, and David S. Cohen. Feature extraction from faces using deformable templates. *International Journal of Computer Vision*, 8(2):99–111, 1992.

[123] Zhengyou Zhang. Iterative point matching for registration of free-form curves and surface. *Int. Journal of Computer Vision*, 1993. to appear, research report available at Inria, Sophia-Antipolis.

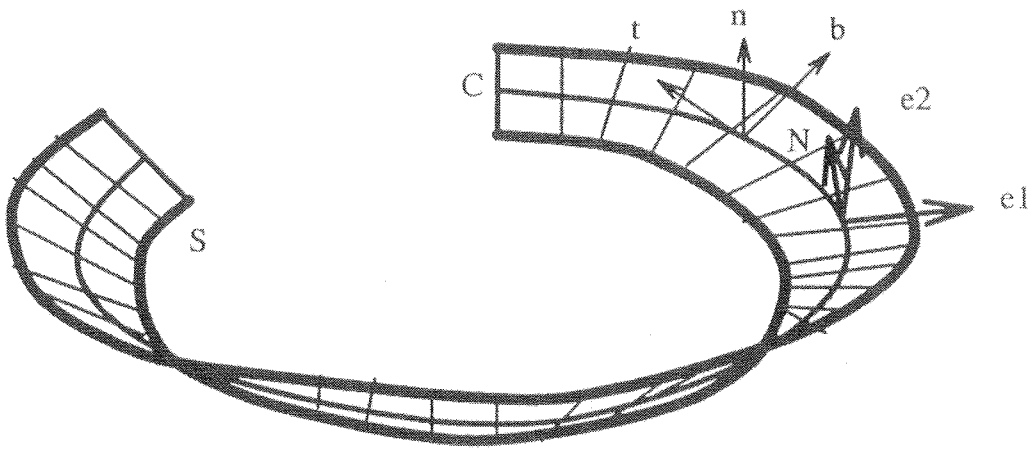

Figure 16: Surface ribbon around a space curve: at each curve point, one can compute the curve Frenet frame (t, n, b), where t and n are respectively the curve tangent and normal, and the local surface frame (e_1, e_2, N), where e_1 and e_2 are the principal directions of curvatures in the tangent plane of the surface, and N the surface normal. (Courtesy of A. Guéziec).

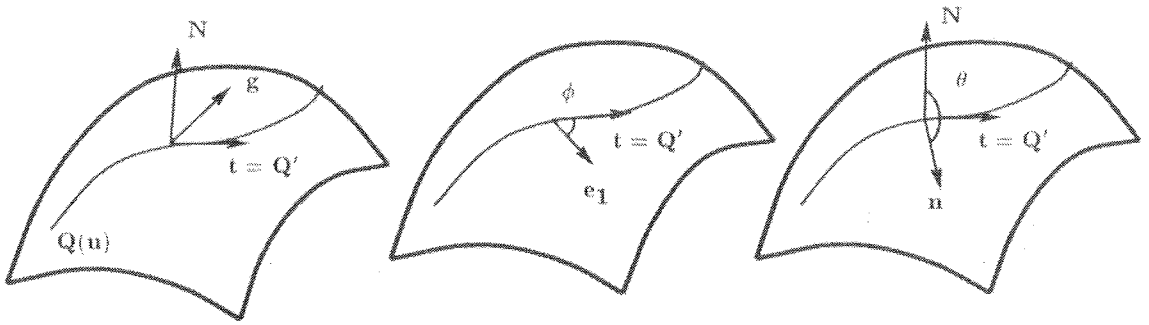

Figure 17: Left: Darboux frame (t, N, g) computed along the ridge line, on the surface. Middle: ϕ is the angle between the direction e_1 of the largest principal curvature k_1 with t. Right: θ is the angle between the curve normal n and the surface normal N. (Courtesy of A. Guéziec).

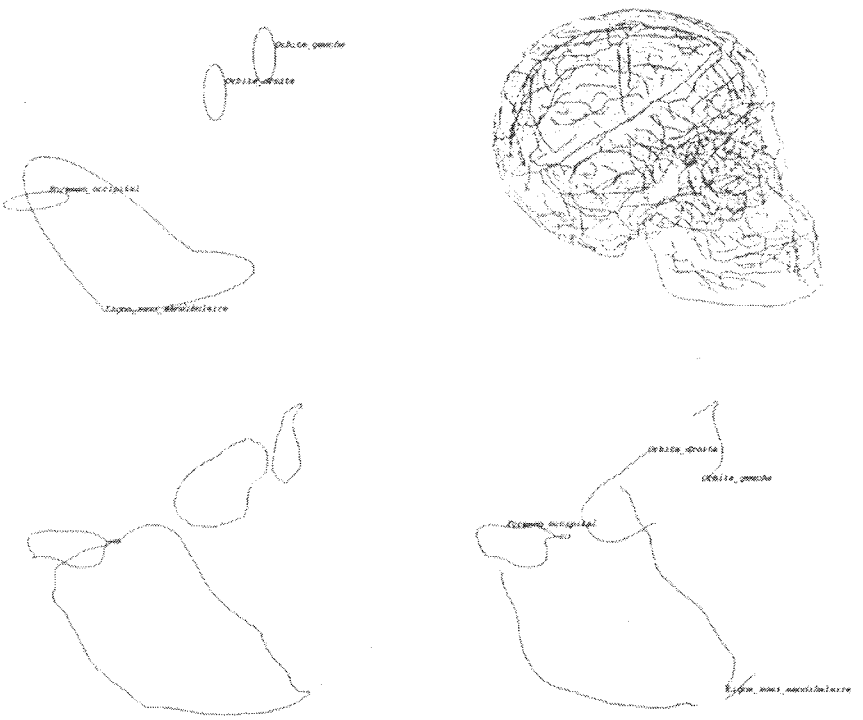

Figure 18: (a) Simplified geometric "atlas" based on a few characteristic ridges placed in "mean" position; (b) Ridges of Arthur; (c) Automatic convergence of the atlas towards the corresponding ridge lines of Arthur; (d) Characteristic ridges of Arthur are now labelled with correct anatomical names. (Courtesy of G. Subsol and J.P. Thirion)

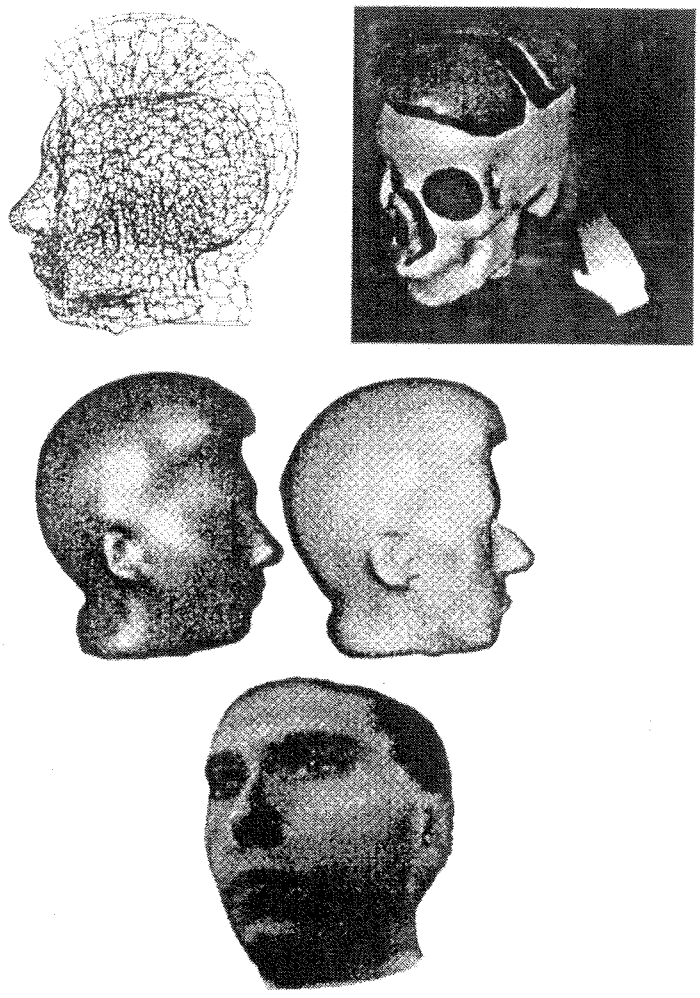

Figure 19: Top Left: an elastic model of the head is designed from the 3D image of the head. Top Right: the skull is cut and its shape is modified with a virtual 3D hand. Middle and Bottom: the elastic model of head of the patient deforms itself accordingly to the modified shape of the skull, and the expected result (a deformed Herve Delingette!) can be observed (possibly with texture) before any real surgery is done. (Courtesy of H. Delingette, G. Subsol, S. Cotin and J. Pignon).